

A numerical model and associated calorimeter for predicting temperature profiles in mass concrete

Yunus Ballim *

Department of Civil Engineering, University of the Witwatersrand, Private Bag 3, WITS, 2050 Johannesburg, South Africa

Received 5 August 2002; accepted 9 May 2003

Abstract

This paper describes the development and operation of a finite difference heat model for predicting the time-based temperature profiles in mass concrete elements. The model represents a two-dimensional solution to the Fourier heat flow equation and runs on a commercially available spreadsheet package.

An important problem facing heat modelling of concrete is that the rate of heat evolution at any point in the concrete element depends on concrete mixture parameters, time and position within the element. The present model resolves much of this complexity by using, as input, the results of a heat rate determination using a low-cost adiabatic calorimeter together with the Arrhenius maturity function to indicate the rate and extent of hydration at any time and position within the structure, based on the time-temperature history at that point.

The paper presents a discussion of the structure of the finite difference model and its application to spreadsheet architecture. A brief description of the calorimeter is also presented together with the results of a verification exercise that was carried out to assess the accuracy of the model using a block of concrete instrumented with thermal probes. The results show that the model is able to predict the temperature at any point in the concrete block to within 2 °C of the measured values.

© 2003 Elsevier Ltd. All rights reserved.

Keywords: Mass concrete; Hydration; Temperature; Maturity; Finite difference; Heat; Adiabatic calorimetry

1. Introduction

This paper discusses the development of a finite difference (FD) numerical model for predicting the temperature at varying times and locations in a mass concrete element. The model is applicable to rectangular concrete elements, which is typical of the construction of large concrete structures such as dams and foundations. The model is a 2-dimensional solution of the Fourier equation for heat flow in solid bodies and, as presently structured, is also simple enough to be programmed into a commercially available spreadsheet software.

In normal concrete construction, the heat developed by the hydrating cementitious materials is quickly dissipated to the environment and this usually poses no serious problems. However, in large or mass concrete elements, thermally induced early-age cracking is a

problem requiring special attention at the design and construction stages. During the early stages of hydration, when the internal temperature of the immature concrete is increasing, the cooler surface zone is subjected to tensile stresses and surface cracks, usually fairly shallow, may occur within a few days after casting. At later ages, after the peak temperature has been reached and the internal concrete enters the cooling phase, the increased stiffness of the surface zone now acts as a restraint to the thermal shrinkage of the internal concrete. Internal sections are, therefore, subjected to tensile stresses and significant internal cracking is possible.

A number of models have been proposed to predict the heat evolution and resulting temperature development characteristics in concrete during the early stages of hydration. These models are either developed at the micro-level for the study of physico-chemical processes associated with the hydration of cement [1], or they are developed at the macro-level for predicting the temperature development in (usually mass) concrete structures. These macro-level models are in the form of graphical

* Tel.: +27-11-717-7104/7110; fax: +27-11-339-1762.

E-mail address: ballim@civil.wits.ac.za (Y. Ballim).

methods [2], manual step-wise calculations [3] or fairly sophisticated finite element methods [4]. The macro models are aimed at providing a tool in the design and construction of mass concrete elements to determine aspects such as suitable cooling systems to be used in the structure, construction sequencing, joint grouting times and the potential for thermally induced concrete cracking. In this sense, the model proposed in this paper is also a macro model since its primary aim is to predict the time-temperature profiles in mass concrete structures.

The potential for concrete to crack depends on a wide range of inter-connected intrinsic and extrinsic factors [5]. Of these, a fundamental factor is the time-based temperature profiles in the concrete structure. An accurate and thorough understanding of the temperature differences occurring in the concrete at different times (as the physical properties change and evolve) is essential for a proper analysis of cracking potential.

An important problem facing heat modelling of concrete is that the rate of heat evolution at any point in the concrete element is dependent on the specific cementitious binder, aggregate type and mixture proportions used in the concrete as well as the extent and rate of hydration at each point in the concrete element at a particular time under consideration. Furthermore, the extent and rate of hydration at any time depends on the historical time and temperature conditions at the particular point in the structure under consideration. The model presented resolves much of this complexity by incorporating the results of a rate of heat evolution determination using a low-cost adiabatic calorimeter. A small sample of the actual concrete to be used is placed in the calorimeter and the temperature rise is monitored over a period of up to 7 days. These results are then used to determine the maturity rate of heat evolution (rather than the time rate) and the time scale of the test is converted to a maturity scale to indicate the extent of hydration. The finite difference model uses this heat rate-maturity relationship to determine the rate of heat evolution at various times and locations in the concrete element, and hence determines the temperature profiles in the element. The Arrhenius maturity function is used in this application.

Finally, the paper presents the results of a verification exercise which was carried out to assess the accuracy of the model and the suitability of the Arrhenius maturity function in this context. A block of concrete was cast and instrumented with thermal probes. The temperature at various points in the block was monitored until the temperature at the centre of the block returned to the ambient temperature. A brief description is also presented regarding the manufacture and use of a thermal probe that uses a temperature sensitive integrated circuit unit, connected to doubly-insulated cable bonded in epoxy. These probes are sufficiently inexpensive (ap-

proximately £1 each) to be discarded after being cast into concrete for the purpose of temperature monitoring.

2. Development of the heat model

The flow of heat in concrete can be described by the Fourier equation which, in its two-dimensional form, is given as [6]:

$$\rho C_p \frac{\partial T}{\partial t} = k \left(\frac{\partial^2 T}{\partial x^2} + \frac{\partial^2 T}{\partial y^2} \right) + Q' \quad (1)$$

where ρ is the density of the concrete; C_p , the specific heat capacity; T , the temperature; t , the time; k , the thermal conductivity; x, y are the coordinates at a particular point in the structure; and Q' , the rate of internal heat evolution.

Eq. (1) was solved numerically for a rectangular block of concrete which has a z dimension significantly larger than the x and y dimensions. As shown in Fig. 1, the block was cast onto a rock foundation and the ambient temperature (T_A) varies with time.

The numerical solution of Eq. (1) is presented in a number of standard texts [6–8]. However, for clarity, a basic introduction to the finite difference (FD) approach used in this analysis is presented below, together with the final form of the FD equations for the different positions in the concrete block and associated boundary conditions.

2.1. Developing the finite difference equations

Fig. 2 shows three internal nodes in an element of material subjected to one-dimensional heat flow. In developing a numerical solution to the one-dimensional form of Eq. (1), the second derivative of the temperature

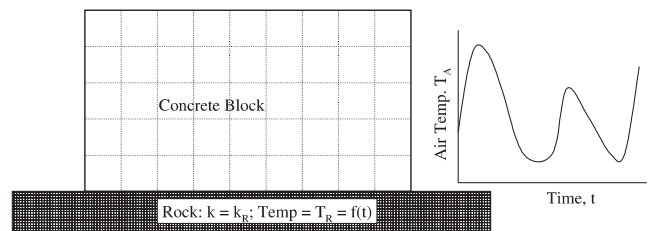


Fig. 1. Schematic arrangement of the modelled mass concrete block.

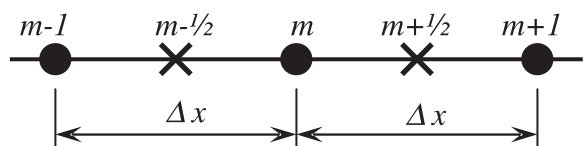


Fig. 2. Three internal nodes in a one-dimensional heat flow arrangement.

(T) with respect to position (x) at point m can be approximated from the FD expression [8]:

$$\left[\frac{\partial^2 T}{\partial x^2} \right]_m \cong \frac{\left[\frac{\partial T}{\partial x} \right]_{m+\frac{1}{2}} - \left[\frac{\partial T}{\partial x} \right]_{m-\frac{1}{2}}}{\Delta x} \quad (2)$$

The first derivatives at the intermediate points are approximated to by

$$\left[\frac{\partial T}{\partial x} \right]_{m+\frac{1}{2}} \cong \frac{T_{m+1} - T_m}{\Delta x} \quad \text{and} \quad \left[\frac{\partial T}{\partial x} \right]_{m-\frac{1}{2}} \cong \frac{T_m - T_{m-1}}{\Delta x} \quad (3)$$

Combining Eqs. (2) and (3) gives

$$\left[\frac{\partial^2 T}{\partial x^2} \right]_m \cong \frac{T_{m+1} + T_{m-1} - 2T_m}{(\Delta x)^2} \quad (4)$$

Also, the rate of change of temperature with respect to time (t) at point m in the time interval: $t = n$ to $t = n + 1$, of duration δt , can be approximated to by

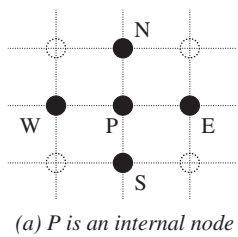
$$\frac{\partial T}{\partial t} \cong \frac{T_m^{n+1} - T_m^n}{\delta t} \quad (5)$$

By extending the principles illustrated in Eqs. (4) and (5) to a two-dimensional heat flow condition, appropriate FD equations were developed for the concrete block shown in Fig. 1. Fig. 3 shows the different node positions for which the FD equations were developed. These equations are presented below.

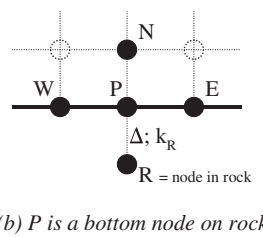
2.2. Internal nodes (Fig. 3(a))

The FD equation for an internal node is

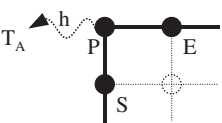
$$T_P^{n+1} = \frac{Q^n \delta t}{\rho C_p} + T_P^n (1 - 4F_0) + F_0(T_N^n + T_E^n + T_S^n + T_W^n) \quad (6)$$



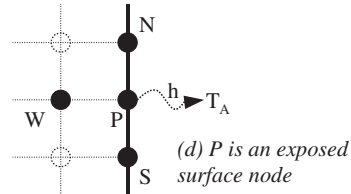
(a) P is an internal node



(b) P is a bottom node on rock



(c) P is a corner node



(d) P is an exposed surface node

Fig. 3. Node positions and boundaries for which FD equations were set up.

$$\text{subject to : } \delta t \leq \frac{\rho C_p \Delta^2}{4k} \quad (7)$$

where, in addition to the parameters defined before, T_X^n is the temperature at node X in the n th time interval; Q^n is the rate of internal heat evolution in the n th time interval; δt is the time-step interval used in the FD analysis; C_p is the specific heat capacity of the concrete, determined as the mass weighted average of the specific heat capacity of each component in the concrete mixture; F_0 is the Fourier number, which is defined as

$$F_0 = \frac{k \delta t}{\rho C_p \Delta^2} \quad (8)$$

and $\Delta = \Delta_x = \Delta_y$ is the distance between nodes. The limitation on δt in Eq. (7) is to ensure stability of the FD model.

2.3. Bottom surface nodes (Fig. 3(b))

A fictitious node R is included in the system at a distance Δ from P and the thermal conductivity of the rock is k_R . The governing equation is then of the form:

$$T_P^{n+1} = \frac{Q^n \delta t}{\rho C_p} + T_P^n \left[1 - F_0 \left(4 + 2 \frac{k_R}{k} \right) \right] + F_0 \left(2T_N^n + T_E^n + T_W^n + 2 \frac{k_R}{k} T_R^n \right) \quad (9)$$

$$\text{subject to : } \delta t \leq \frac{\rho C_p \Delta^2}{k \left(4 + 2 \frac{k_R}{k} \right)} \quad (10)$$

In the absence of direct solar radiation, the temperature response of materials such as rock, to variations in the ambient temperature, is slow. The temperature of the rock at node R, T_R^n , is therefore taken as the minimum temperature occurring on the previous day.

2.4. Corner nodes (Fig. 3(c))

In this case, heat is also transferred between node P and the environment by conduction and the rate of such transfer is determined by the heat transfer coefficient h . The governing equation is then:

$$T_P^{n+1} = \frac{Q^n \delta t}{\rho C_p} + T_P^n [1 - 4F_0(1 + B_i)] + 2F_0(T_E^n + T_S^n + 2B_i T_A^n) \quad (11)$$

$$\text{subject to : } \delta t \leq \frac{\rho C_p \Delta^2}{4k(1 + B_i)} \quad (12)$$

where T_A is the ambient temperature and B_i is the Biot number, which is defined as

$$B_i = \frac{h \Delta}{k} \quad (13)$$

2.5. Exposed surface nodes (Fig. 2(d))

For the corner nodes, heat is transferred to the environment and the FD equation is

$$T_{\text{P}}^{n+1} = \frac{Q^n \delta t}{\rho C_p} + T_{\text{P}}^n \left[1 - 4F_0 \left(1 + \frac{1}{2} B_i \right) \right] + F_0 (2T_{\text{W}}^n + T_{\text{N}}^n + T_{\text{S}}^n + 2B_i T_{\text{A}}^n) \quad (14)$$

$$\text{subject to : } \delta t \leq \frac{\rho C_p \Delta^2}{(4k + 2h\Delta)} \quad (15)$$

In selecting the time interval (δt) for the operation of the finite difference model, the minimum of the values for δt generated by Eqs. (7), (10), (12) and (15) should not be exceeded to ensure overall stability of the model.

2.6. Modelling the environmental temperature T_A

At the design stage of a construction project, it is unlikely that accurate and continuous ambient temperature values are available for the area in which the construction is to take place. This is more so because temperature values are required at approximately 1-h intervals. However, daily ambient maximum and minimum temperatures are usually available from the local meteorological office and a model was developed to approximate the ambient temperature at any time using only the daily maximum and minimum values. This model takes the form:

$$T_A = -\sin \left(\frac{2\pi(t_d + t_w)}{24} \right) \left(\frac{T_{\max} - T_{\min}}{2} \right) + \left(\frac{T_{\max} + T_{\min}}{2} \right) \quad (16)$$

where: t_d is the clock time of day at which the approximation is being made (0–24 h); t_w is the time at which the minimum overnight temperature occurs (usually just at sunrise); T_{\max} and T_{\min} are, respectively, the maximum and minimum temperatures for the day under consideration. The model represented by Eq. (16) is a sinusoidal function with a 24-h period and variable amplitude ($T_{\max} - T_{\min}$). t_w is a shift factor, which allows the time of the minimum temperature to be correctly adjusted.

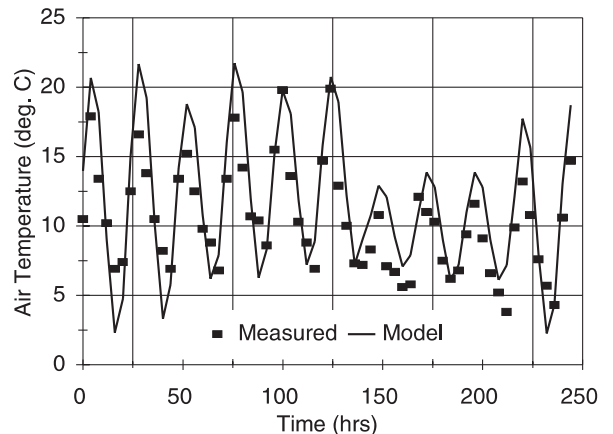


Fig. 4. Measured air temperature compared to the modelled values using Eq. (16).

The ambient temperature model is over-simplified in that it ignores factors such as cloud cover, wind or direct sunlight and there is probably room for significant refinement. Nevertheless, Fig. 4 shows that the model gives reasonably good prediction when compared with actual measured outdoor temperatures over a trial period of 10 days.

2.7. Determining the rate of internal heat evolution, Q'

An adiabatic calorimeter was developed and built to measure the rate of heat evolution of a concrete mixture to be used in the construction of the concrete element. Details of the construction and operation of the calorimeter are given by Gibbon et al. [9] and Gibbon and Ballim [10]. A schematic arrangement of the calorimeter is presented in Fig. 5. In principle, the test involves placing a one litre sample of concrete in a water bath, such that a stationary pocket of air separates the concrete sample from the water. The signal from a thermal probe placed in the sample is monitored by a desk-top computer and, via an input/output analogue to digital conversion card, the heater in the water bath is turned on and off so as to maintain the water at the same temperature as the concrete. This ensures that there is no exchange of heat between the concrete sample and

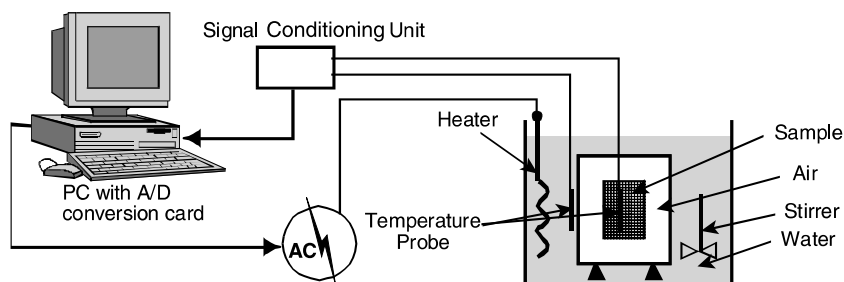


Fig. 5. Schematic arrangement of the adiabatic calorimeter.

the surrounding environment. The pocket of air around the sample is important to dampen any harmonic response between the sample and water temperature as a result of the measurement sensitivity of the thermal probes. The test is usually run over a period of between 5 and 7 days, by which time the rate of heat evolution of the sample is too low to be detected as a temperature difference by the thermal probes—given that the thermal probes are accurate to approximately 0.5 °C.

The test measurement produces a curve of temperature vs. time for a particular binder type and mixture composition. The total heat evolved over any time period can be determined from the relationship:

$$Q = mC_p \delta T \quad (17)$$

where m is the mass of the sample and δT is the change in temperature of the sample over the time period under consideration. The rate of heat evolution is then determined from a numerical differentiation with respect to time (t) of the total heat curve, i.e.:

$$\dot{Q}_t = \frac{\partial Q}{\partial t} \quad (18)$$

However, Eq. (18) yields a rate of heat evolution which is unique to the conditions under which the adiabatic test was conducted. In determining the cumulative heat produced by the binder, Eq. (17) is only concerned with temperature differences and not absolute temperatures. As a chemical reaction, the rate and extent of hydration is influenced by the absolute temperature under which the reactions take place. In principle, therefore, each point in a concrete structure that is subjected to a unique time–temperature profile will exhibit a unique time–heat rate profile.

This is contrary to past approaches where the form of the time-based heat of hydration curve ($Q = f(t)$) was considered as fixed [11]. Wang and Dilger [12] use this approach to the heat rate form and propose the following equation for determining the rate of heat evolution (in W/kg of cement) to be used in Eq. (1):

$$\begin{aligned} \frac{\partial Q}{\partial t} &= 0.5 + 0.54M^{0.5} \quad \text{for } M \leq 10 \text{ h} \\ &= 2.2 \exp[-0.0286(M - 10)] \quad \text{for } M \geq 10 \text{ h} \end{aligned} \quad (19)$$

where M is the equivalent age or maturity of the concrete referenced to concrete cured at 20 °C. Eq. (19) express the time-based heat rate in terms of the development of maturity, with a fixed maximum heat rate of 2.2 W/kg. Clearly, this approach cannot be considered as appropriate for a concrete temperature prediction model since:

- The maximum heat rate is determined by the temperature at which the hydration takes place and, therefore, cannot be considered as constant;

- Hypothetically, if the temperature of the concrete in the structure is reduced to –10 °C, when hydration is deemed to cease [13], the maturity remains constant hereafter and Eq. (19) predicts a finite rate of heat evolution when, in fact, the heat rate has reduced to zero.

In order to address this problem, it is necessary to express the heat evolved as measured in the adiabatic test in terms of the a “maturity heat rate” as a function of the cumulative maturity, rather than a time rate. The maturity heat rate (\dot{Q}'_M) is expressed as

$$\dot{Q}'_M = \frac{dQ}{dM} \quad (20)$$

and the time-based heat rate, as required in Eq. (1), is then determined using the chain rule as follows:

$$\dot{Q}'_t = \dot{Q}'_M \cdot \frac{dM}{dt} \quad (21)$$

Hence, a temperature prediction model for concrete should use, as input, the calculated maturity and corresponding maturity heat rate determined from the adiabatic calorimeter test. It is then necessary for the model to maintain a measure of both the development of maturity and the time based rate of change of maturity at each point under consideration in the concrete element. At each calculation step, an appropriate maturity heat rate is selected, based on the cumulative maturity at the point under consideration. Multiplying by the time-based rate of change of maturity in the given time interval, yields the time-based heat rate to be used in the solution of Eq. (1).

The form of the heat rate expression as presented in Eqs. (20) and (21) also address the problem presented above, where the temperature of the concrete is suddenly reduced to point where the hydration ceases. In this case, the time-rate of change of maturity is zero and Eq. (21) correctly yields a \dot{Q}'_t value of zero.

A number of maturity functions have been proposed [12–14], mainly with a view to predicting the strength of concrete under different curing temperature conditions. For this investigation, it was decided to use the Arrhenius maturity function to determine the equivalent age of a concrete with respect to concrete continuously cured at 20 °C (Eq. (22)). In consideration of compressive strength prediction, Naik [13] demonstrates the appropriateness of the Arrhenius function and cautions strongly against using the Nurse–Saul expression.

The modified expression for the equivalent age, based on the Arrhenius relationship, is given as [13]:

$$t_{20} = \sum_{i=1}^n \exp \left[\left(\frac{E}{R} \right) \left(\frac{1}{273 + T_0} - \frac{1}{T_i} \right) \right] \Delta t_i \quad (22)$$

where t_{20} is the time required, when curing at 20 °C, to reach an equivalent maturity; T_i is the average concrete

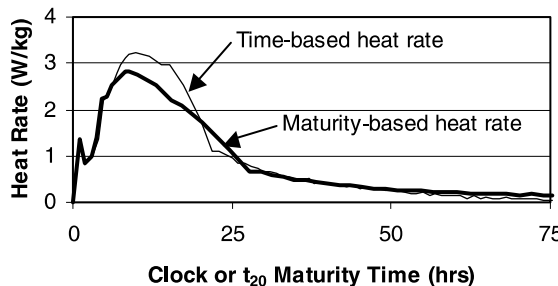


Fig. 6. Rates of heat evolution of a sample concrete under adiabatic conditions expressed in terms of clock time- and equivalent Arrhenius maturity time.

temperature (in K) in the time interval Δt_i ; T_0 is the reference temperature (taken as 20 °C); E is the apparent activation energy (taken as 33.5 kJ/mol [15]) and R is the universal gas constant (8.31 J/mol K).

Fig. 6 shows the time- and maturity-based rates of heat evolution of the concrete used in the verification exercise of this study (discussed later). For the maturity-based heat rate, the age axis is expressed in terms of t_{20} h using Eq. (22). In determining the adiabatic temperature rise of this concrete, the test was started at 18 °C and the concrete reached a maximum temperature of 36 °C after approximately 80 h in the calorimeter.

Fig. 6 also shows that the generalised heat rate-maturity expressions proposed by Wang and Dilger [12] would under-estimate the heat rate for this concrete. Their expression indicates a maximum heat rate of 2.2 W/kg while the maximum time-based value determined from this test was 3.21 W/kg and the maximum maturity-based value was 2.83 W/kg. Care should be taken in comparing the two curves shown in Fig. 6 since the horizontal axis does not relate to the two curves in a linear manner. As an illustration, the test was terminated after 80 clock hours and, at this stage, the equivalent maturity age was 143 t_{20} h. Nevertheless, it is clear that, in this case, using the same time-based heat rate curve in the model throughout the section will overestimate the temperatures developed in the concrete. The maturity-based heat rate curve shown in Fig. 6 was used as input into the numerical model discussed below.

2.8. Application of the model to spreadsheets

With the increased sophistication of spreadsheet architecture and programming ability, it was found that the FD model could easily be programmed as a “macro” in a spreadsheet. The normal two-dimensional structure of a page and three-dimensional structure of a “work-book” lends itself particularly well to the step-wise calculation requirements of the model. Also, the “look-up” feature in these spreadsheets allows the user to install data sets of (say) maturity heat rate and corresponding maturity. The programme will then select an appropri-

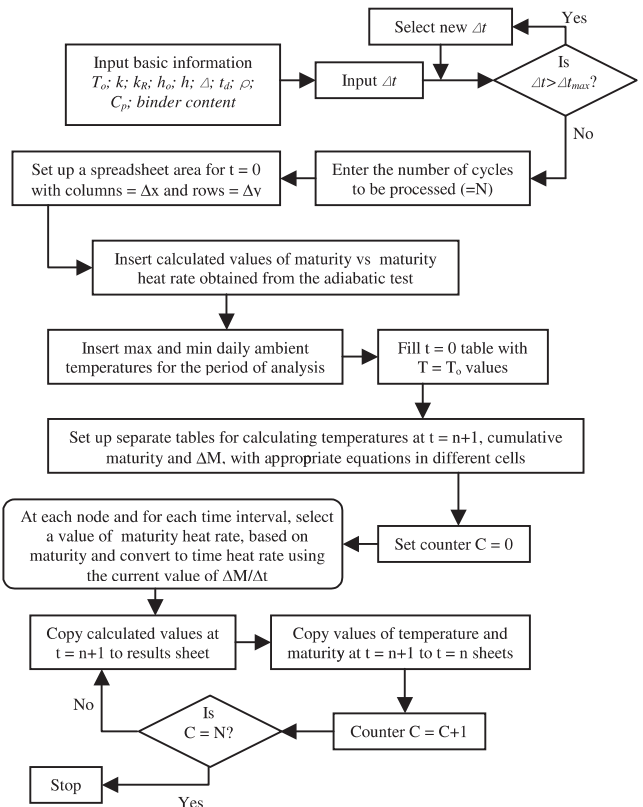


Fig. 7. Flow diagram for the finite difference computer programme.

ate value of heat rate on the basis of a calculated value of maturity. A similar procedure can be set up if the thermal conductivity of the concrete is known to vary with time and degree of hydration, as has been noted by some researchers [14]. The general programme flow diagram is shown in Fig. 7. It should be noted that, for the situation as shown in Fig. 1, the section is symmetrical about the vertical axis and the equations need only be solved for one half of the concrete element under consideration.

3. Laboratory verification of the proposed model

A block of concrete was cast in the laboratory and instrumented with thermal probes in order to assess the accuracy of the proposed model. The block, comprising 0.5 m³ of concrete was cast with dimensions as shown in Fig. 8(a). The concrete used in the block had a nominal compressive strength of 25 MPa, a maximum aggregate size of 13 mm, a slump of 100 mm and the binder consisted of portland cement (220 kg/m³). The slump and aggregate size were selected to ensure that the thermal probes were not displaced during casting. The block was cast onto a concrete floor in the laboratory and the formwork for the two 700 × 700 mm surfaces

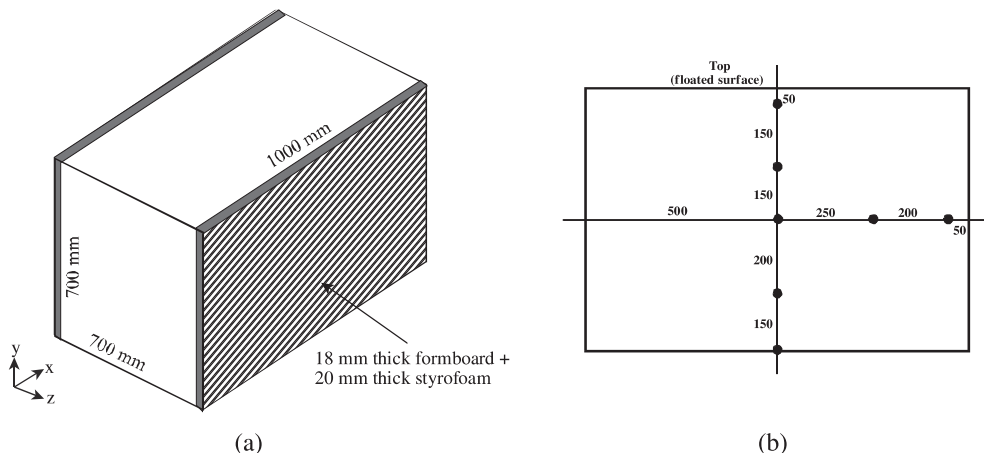


Fig. 8. Showing (a) the concrete test block with side insulation and (b) location of the thermal probes in the centre of the block on an $x-y$ plane.

was removed at 18 h after casting. These surfaces were then coated with a wax-based curing compound.

As indicated in Fig. 8(a), the block was insulated on the two opposite 700×1000 mm faces in order to approximate two-dimensional heat flow. Thermal probes were placed in the concrete at the node points shown in Fig. 8(b) and these were held in place by being tied to a network of thin nylon line attached to the insides of the formwork. A probe was also placed on the outside of the concrete block to monitor the ambient temperature. The thermal probes were manufactured from integrated circuit (ic) units that required a dc input voltage of 10 V and had an output of 0–1 V, representing a temperature of 0–100 °C. The ic units were connected to doubly insulated telephone cable and this assembly was encased in epoxy, to form a probe measuring 6 mm in diameter and approximately 40 mm long. The total cost of a completed probe was approximately £1 (UK). The calibration of each probe was assessed over a range of 10–60 °C and, where necessary, correction factors were applied to the measured output signals.

The probes were connected to an automatic data-logging facility and a constant voltage supply unit. Voltage signals at each of the probes were recorded at 1-h intervals up to 90 h after casting, by which time the temperature at the centre of the block had returned to ambient. During this period, the ambient temperature varied between 16 and 21 °C.

At the time of casting, a small sample of the concrete was obtained for the adiabatic calorimeter test, which was conducted at the same time as the temperature monitoring of the test block. The calculated rate of heat evolution for this concrete with respect to clock time and Arrhenius maturity time is shown in Fig. 6. These curves were used as input for the FD model. The thermal conductivity of the concrete was taken as 3.5 W/m K (as recommended for quartzite aggregate concretes [14]); based on a mass weighted average [2], the specific heat of

the concrete was calculated to be 1228 J/kg K. The heat transfer coefficient was estimated from research work reported in Ref. [9] and was taken as 30 W/m² K for exposed concrete surfaces and 5 W/m² K for the 700×700 mm end surfaces over the first 18 h while they were covered by formwork timber. The analysis was done in 30-min time steps with $\Delta x = \Delta y = 100$ mm.

4. Results and discussion

As an illustration, the results obtained at six of the probe locations are shown in Fig. 9. These figures also show the results of the model predictions at corresponding locations using the Arrhenius maturity function. The results show that the temperature of the concrete started at approximately 17 °C, reached a peak of 28 °C at the centre of the block and returned to ambient temperature at approximately 80 h after casting.

Fig. 9 shows that the FD model is able to predict the temperature to within 2 °C throughout the temperature monitoring period. For the central node, the model predicts the maximum temperature reasonably well but the predicted time of occurrence of the maximum temperature is slightly later than the measured time. The largest deviation between the predicted and measured values occurs for the nodes close to the surface, as can be seen in the lower part of Fig. 9. When the concrete surface is exposed directly to the surrounding environment, not only is the measured temperature lower than the prediction (by up to 2 °C) but the concrete is also not responding to ambient temperature variations as strongly as the model results indicate. This situation occurs immediately after casting for the top surface and after the side formwork was removed from the side surfaces. A possible reason for this deviation is an error in estimation of parameters such as the thermal

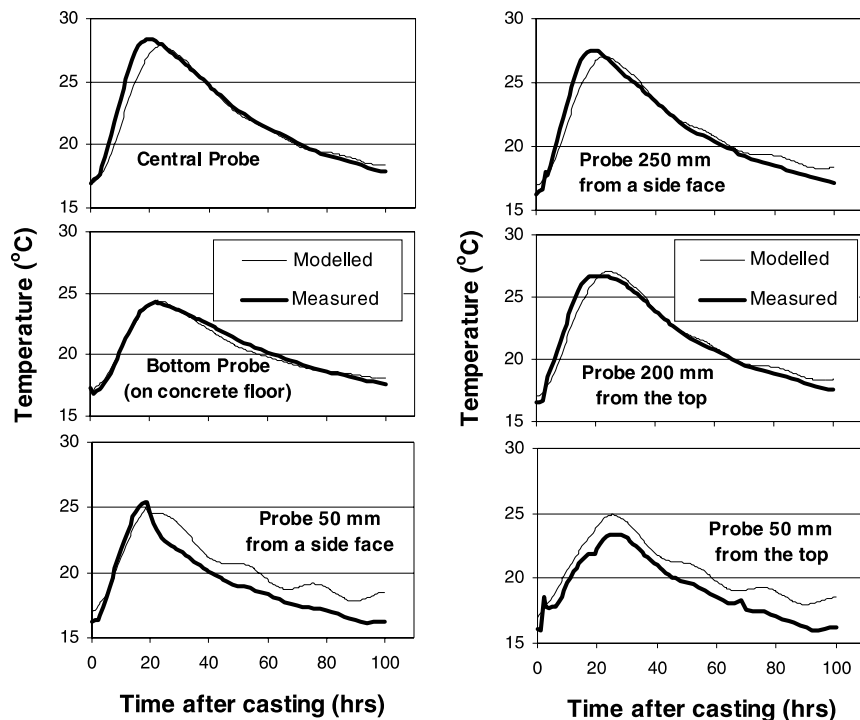


Fig. 9. Modelled and measured temperatures at six of the probe positions.

conductivity and the coefficient of heat transfer. A further possible reason is that, despite the application of the curing compound, the concrete had dried out near the surface and this caused the hydration to cease in this zone. The rate of heat evolution at this point was therefore lower than the model predicted from the maturity calculation and this resulted in an over-estimate of the temperature at this node. The loss of moisture would also have had the effect of reducing the thermal conductivity of the surface zone and this would explain the lack of sensitivity of this node to variations in ambient temperature. Fig. 9 also shows that the model is able to simulate the sudden drop in temperature as a result of the removal of the formwork from the side surfaces after 18 h.

Notwithstanding these observations, given the simplicity and low-cost of the model and its operation, the results are promising. It is intended that future work in this area will be aimed at developing the model to allow for the effects of sequential construction—casting fresh concrete onto concrete from which some or all the heat has not yet been lost.

Furthermore, using an ever growing database of heat rate curves for different cementitious binder types, it is possible to assess the likely effects of different binder types on the temperature development within a particular concrete element for given environmental conditions. The model can therefore be used as a valuable tool in the selection of the concrete mixture proportions before construction commences. The model can also be

used to assess the efficacy of a reduced concrete mixture temperature, which is normally achieved by using flaked ice as mix water or by injecting liquid nitrogen into the fresh concrete mix.

5. Conclusions

- As described, the spreadsheet-based finite difference model provides a low-cost and reasonably accurate means for predicting the time-based temperature profiles in mass concrete structures where potential cracking may present a problem.
- The adiabatic test together with the Arrhenius maturity function allows for the rate of heat evolution from the hydrating cement to be expressed in a rational and normalised form for input into the numerical model. The heat rate must be expressed in the form of a maturity heat rate as a function of the cumulative maturity of the concrete. In the step-wise analysis of the model, it is important to maintain an incremental measure of the cumulative maturity at each point under analysis as well as a measure of the time rate of change of maturity at each point.
- It appears that early drying from the surface of the concrete causes inaccuracies in the ability for the model to estimate concrete temperatures near the surface. This points to a need for improved definition of the boundary conditions of the model, in-

cluding an accurate assessment of parameters such as the heat transfer coefficient.

Acknowledgements

Sincere thanks are due to Mr. M.T. Mokonyama and Mr. P. Tshabalala for their assistance with the casting of the concrete block and the initial reduction of the results.

References

- [1] Garboczi EJ, Bentz DP. Computer-based models of the microstructure and properties of cement-based materials. In: Proceedings of ninth International Conference on the Chemistry of Cement, New Delhi, Vol. VI, 1992. p. 3–15.
- [2] Addis BJ, editor. Fulton's concrete technology. 6th Revised Edition. Portland Cement Institute, Midrand, South Africa, 1986, 956 pp.
- [3] United States Bureau of Reclamation: Control of cracking in mass concrete structures. Engineering Monograph no. 34, The Bureau, Denver, 1965.
- [4] Kishi T, Maekawa K. Thermal and mechanical modelling of young concrete based on hydration process of multi-component cement minerals. In: Springenschmid R, editor. Thermal cracking in concrete at early ages. London: E&FN Spon; 1994. p. 11.
- [5] Andersen ME. Design and construction of concrete structures using temperature and stress calculations to evaluate early-age thermal effects. In: Skalny J, Mindess S, editors. Materials Science of Concrete, vol. 5. American Ceramic Society; 1998. p. 191–263.
- [6] Holman JP. Heat transfer. 7th ed. New York: McGraw Hill; 1990. 714 pp.
- [7] Dusinberre GM. Heat transfer calculations by finite differences. Pennsylvania, US: International Textbook Company; 1961. 293 pp.
- [8] Croft DR, Lilley DG. Heat transfer calculations using finite difference equations. London: Applied Science Publishers; 1977. 283 pp.
- [9] Gibbon GJ, Ballim Y, Grieve GRH. A low-cost, computer-controlled adiabatic calorimeter for determining the heat of hydration of concrete. *J Testing Evaluat (ASTM)* 1997;25(2):261–6.
- [10] Gibbon GJ, Ballim Y. Laboratory test procedures to predict the thermal behaviour of concrete. *J South African Inst Civil Engineers* 1996;38(3):21–4 (3rd Quarter).
- [11] Clover RE. Calculation of temperature distribution in a succession of lifts due to release of chemical heat. *J ACI* 1937;34:105–16.
- [12] Wang CH, Dilger WH. Prediction of temperature distribution in hardening concrete. In: Springenschmid R, editor. Thermal cracking in concrete at early ages. London: E&FN Spon; 1994. p. 21–8.
- [13] Naik TR. Maturity functions for concrete cured during winter conditions. In: Naik TR, editor. Temperature effects on concrete, ASTM STP 858. Philadelphia: American Society for Testing and Materials; 1985. p. 107–17.
- [14] Van Breugel K. Prediction of temperature development in hardened concrete. In: Springenschmid R, editor. Prevention of thermal cracking in concrete at early ages, RILEM Report 15. London: E&FN Spon; 1998. p. 51–75.
- [15] Bamford CH, Tipper CFH, editors. The practice of kinetics. Comprehensive chemical kinetics, vol. 1. London: Elsevier; 1969.